

Stable Chaos in the 12:7 Mean Motion Resonance and Its Relation to the Stickiness Effect

Kleomenis Tsiganis, Harry Varvoglis, and John D. Hadjidemetriou

Section of Astrophysics, Astronomy, and Mechanics, Department of Physics, University of Thessaloniki, 54006 Thessaloniki, Greece
E-mail: tsiganis@astro.auth.gr

Received April 8, 1999; revised January 24, 2000

We follow the evolution of distributions of real and fictitious asteroids, initially placed in the vicinity of the 12:7 mean motion resonance with Jupiter. Our results show that, besides the well-known example of 522-Helga, other stable chaotic asteroids could, in principle, exist in this region of the belt. Most of the particles, though, attain Jupiter-crossing orbits within 50 Myr, under the influence of other close-by resonances (e.g., 5:3). However, the escape process is also controlled by the initial value of the critical argument $\varpi - \varpi_J$. In this respect 522-Helga can, in fact, be the remnant of a larger initial distribution, as conjectured by M. Murison *et al.* (1994, *Astron. J.* 108, 2323–2329). Numerical indications that quasi-periodic orbits exist among the nonremoved test particles support the idea that stable chaos may be a special realization of what is known in Hamiltonian dynamics as stickiness effect. This is also corroborated by the fact that the autocorrelation function, $r(k)$, of the action time series of stable chaotic orbits is almost a quasi-periodic function, in contrast to escaping orbits, for which $r(k)$ decays exponentially. Implications to the problem of formulating a diffusive approach are also discussed. © 2000 Academic Press

Key Words: asteroids; dynamics; celestial mechanics; chaos.

1. INTRODUCTION

The notion *stable chaos* appeared in the literature of celestial mechanics as a term devised by Milani and Nobili (1992) to describe the peculiar behavior of the asteroid 522-Helga, which lies in the immediate vicinity of the 12:7 mean motion resonance with Jupiter. Briefly this term means that, although the trajectory of Helga is characterized by a short dynamical lifetime, $T_L = 1/\lambda \approx 7000$ years (where λ is the maximal Lyapunov characteristic number), its orbital elements show a remarkable stability over a time interval comparable to the age of the Solar System. This discovery raised some important questions among the astronomical community, especially after a relationship between the dynamical lifetime, T_L , and the *escape time*, T_E , of an asteroid,

$$T_E \sim T_L^a, \quad (1)$$

was reported by Lecar *et al.* (1992); 522-Helga violates this statistical “law.” Murison *et al.* (1994) proposed that 522-Helga

may be the remnant of a much larger distribution of asteroids, initially in the vicinity of the 12:7 resonance, most of which where ejected on hyperbolic orbits within 100 Myr from the formation of the Solar System. This is because, according to their results, for any given value of T_L the escaping distribution is a Gaussian and, for $T_L \sim 7000$ years, the age of the Solar System lies within three standard deviations from the mean escape time. Thus, they concluded, stable chaos, as defined by Milani and Nobili (1992), may be thought of as a “statistical fluctuation” of Eq. (1) and does not constitute a new phenomenon in the dynamical behavior of asteroids. Subsequently, other asteroids exhibiting similar behavior were also found, in several regions of the main asteroid belt (see, e.g., Milani *et al.* 1997, Sidlichovsky 1999).

Varvoglis and Anastasiadis (1996) have shown that Eq. (1) can be recovered through a *diffusive approximation* of the problem, i.e., the solution of a suitably modified Fokker–Planck equation,

$$\frac{\partial f(I, t)}{\partial t} = D \frac{\partial^2 f(I, t)}{\partial I^2} - \frac{f(I, t)}{T_E}, \quad (2)$$

which describes the diffusion in action (eccentricity) of an initial distribution of asteroids, $f(I)$, provided that $D = a\lambda^b = \text{const}$. This last relation between D and λ was found, numerically, by Konishi (1989) and holds only in the “resonance-overlap regime” of Hamiltonian systems. The agreement between the above two different approaches may be attributed to the fact that, in order to speed up their numerical calculations, Murison *et al.* (1994) increased the mass of the perturber by a factor of 10 with respect to the actual mass of Jupiter, $\mu = 10 \mu_J$, extrapolating their results to the actual Solar System case ($\mu = \mu_J$). However, as the perturbation is proportional to μ , the already small set of invariant tori in the outer part of the asteroid belt was further reduced and the topology of the phase space was drastically modified. In fact, as noted in Murray and Holman (1997), for $\mu = 10 \mu_J$ the 2:1 and 3:2 resonances of the elliptic restricted three-body problem overlap, even for small eccentricities. Thus, a single, connected, chaotic region covers a wide range of semimajor axes (the “outer asteroid belt”). However, in the real Solar System, Eq. (1) cannot hold, since the topology

of the action space is probably far more complex, as discussed in Varvoglis and Anastasiadis (1996), Morbidelli and Froeschlé (1996), and Murray and Holman (1997; see also Holman and Murray 1996).

The complexity of the phase space is what led Varvoglis and Anastasiadis (1996) to conjecture that Helga may be a real-life example of *stickiness*, an effect caused in nearly-integrable Hamiltonian systems by the surviving KAM tori that are immersed in the stochastic sea and other “quasi-barriers” (e.g., *cantori* in 2D—Aubry 1978, Percival 1979) surrounding them; this was also discussed by Murison *et al.* (1994). It has been shown that stickiness results in *anomalous transport* properties (Shlesinger *et al.* 1993, Zaslavsky 1994). If this is true, transport of chaotic trajectories in this subset of action space, in which Helga lies, cannot be modeled as a *normal* (Brownian) *random walk*, as it is supposed in solving Eq. (2), but, instead, the notion of *Lévy walks* (Shlesinger *et al.* 1993) may be more suitable. One, of course, has to demonstrate the existence of quasi-periodic orbits in the immediate vicinity of Helga, which could act as “quasi-barriers” for action diffusion.

Working on the planar elliptic restricted three-body problem, Murray and Holman (1997) have shown that the relation between the Lyapunov time and the escape time in the outer asteroid belt is far more complex than the simple *monotonic* relation reported by Lecar *et al.* (1992), which holds only in the case where the effective perturbation parameter is close to the critical threshold. Moreover, Murray and Holman (1997) derived an analytic approximation of the quasi-linear *diffusion coefficient* for “random-walking” in action space, which (coefficient) is action dependent. Using an approximate solution of the Fokker–Planck equation, they have shown that the escape time for low-eccentric orbits initiated on the 12:7 resonance is comparable to the age of the Solar System, although their Lyapunov time is of the order of 10^4 years. Thus, they concluded, Helga is neither an example of stable chaos nor the remnant of a larger initial distribution; instead, the stable-looking behavior of Helga is due to the slow diffusion from the 12:7 mean motion resonance.

In this paper we study the statistics of escape from the vicinity of the 12:7 mean motion resonance. Our results show that the phase space in this region of the belt is very complicated and the escape time of a test particle may vary by orders of magnitude, depending on the initial conditions. Other “stable chaotic” orbits (i.e., with exactly the same behavior in terms of orbital elements, evolution of the critical argument and the Lyapunov exponent as 522-Helga) are found within our initial distribution. Moreover, we investigate the idea of Varvoglis and Anastasiadis (1996) that the property of stable chaos may be a realization of the stickiness effect in this specific dynamical system. Finally, we show that stable chaotic orbits share a common characteristic: long-time correlated evolution of the actions. The possibility of existence of a statistical “law,” pertaining to asteroidal escape, is also discussed.

In the next section (Section 2), we present the models used and the numerical setup of our integrations. Some basic aspects

of the dynamics in the vicinity of the 12:7 mean motion resonance are presented in Section 3. Our numerical results are presented in Section 4. Finally, in Section 5, we summarize our conclusions and discuss the possible implications of our results to the problem of formulating a proper *diffusive approach* for asteroidal transport.

2. NUMERICAL SETUP

In order to examine the diffusive character of motion for particles initiated at a given subset of the action space, one has to explore thoroughly the conjugate angles’ space. This is because at any given action value, if the perturbation is not well above some “critical” threshold, some initial phases may lead to vastly chaotic behavior, while some others may not. This kind of dependence of the evolution of an asteroid on its initial phase (actually the resonant arguments σ and ν) has already been observed in some cases of resonant motion in the asteroid belt, namely the 3:1 and 2:1 resonances (Hadjidemetriou 1995, Hadjidemetriou and Lemaître 1997). It is related to the existence of stable or unstable resonant periodic orbits, which correspond to different values of the critical arguments. This is exactly what we wish to explore, i.e., which initial phases lead to fast diffusion, which to slow diffusion, and which, if any, lead to stable chaos or regular (quasi-periodic) motion. If initial conditions leading to stable chaotic trajectories gather close to sets of initial conditions which lead to quasi-periodic motion, this would be an indication that *stable chaos* is, indeed, a suitable oxymoron describing what is known in Hamiltonian dynamics as *stickiness effect*.

In this respect, we integrate the equations of motion for two groups of initial conditions. The first group (hereafter G1) is composed of 128 fictitious asteroids having initial conditions $a = a_{12/7}$ AU, $e = 0.07$, $i = 4^\circ$ and $\Omega = 0$, while ω and M are distributed on a 16×8 grid on $S^2 = \{(0, 2\pi) \times (0, 2\pi)\}$, respectively. Following the standard notation of celestial mechanics, a denotes the semimajor axis, e the eccentricity, i the inclination to the invariant plane, Ω the longitude of the ascending node, ω the argument of perihelion and M the mean anomaly of the minor body. In the Delaunay formalism of the restricted three-body problem, the angles M , ω , and Ω are conjugate to the actions $\mathcal{L} = \sqrt{a}$, $\mathcal{G} = \mathcal{L}\sqrt{1 - e^2}$, and $\mathcal{H} = \mathcal{G} \cos(i)$, respectively, where μ is the ratio of the mass of Jupiter to the total mass of the system. Also, we denote by $a_{12/7}$ the value of the semimajor axis corresponding to the 12:7 mean motion resonance, which is defined by the relation

$$a_{(p+q)/p} = a_J \left(\frac{p}{p+q} \right)^{2/3}, \quad (3)$$

where a_J is the semimajor axis of Jupiter and p , q are integers. The second group (G2) contains the “true” Helga, with initial conditions taken for the epoch JD2448601.0 (Dec. 10, 1991) from the paper of Murison *et al.* (1994), and 128 clones of Helga

with initial a , e , i , and Ω equal to those of Helga, while ω and M are again distributed on a 16×8 grid on S^2 . Thus, both distributions are delta-functions of the three actions. The main model used in this study is the spatial elliptic restricted three-body problem (hereafter ERTBP) and the equations of motion are integrated using the regularized mixed variable symplectic integrator *swift_rmvs3*, from the SWIFT package designed by Levison and Duncan (1994), with a time step of 36.525 days. Finally, the effect that all four outer planets, fully interacting, have in the evolution of G2 is also examined (subsequently we refer to this model as 4P). The initial conditions for the planets are taken from the *Astronomical Almanac* (1991).

In the beginning, the equations of motion of every particle are integrated up to 20 Myr, unless it previously suffers a close encounter with Jupiter, i.e., it passes within Hill's radius from the planet. In this case the integration is stopped, assuming that the "asteroid" will be swiftly ejected from the system. The integration continues up to 50 Myr for all G2 particles that are not ejected within the first 20 Myr. A 5-Gyr integration is also done for 522-Helga alone, in order to verify the results of Milani and Nobili (1992) and Murray and Holman (1997), which have shown that the orbital lifetime of 522-Helga is comparable to the age of our Solar System.

3. DYNAMICS IN THE 12:7 MEAN MOTION RESONANCE

The knowledge of the dynamics of the model we use is essential in understanding the evolution of the system. We shall present briefly in this section the main aspects of the dynamics inside the 12:7 mean motion resonance, in which 522-Helga is verified to lie. A full exploration of the phase space is beyond the scope of this paper.

3.1. Circular Planar Restricted Three-Body Problem

The basic model we shall start with is the planar circular restricted three-body problem (Sun–Jupiter–asteroid). Although this is not a realistic model, it contains the basic features of the complete model and, for this reason, it is very useful in understanding the dynamics of more realistic models (e.g., elliptic orbit of Jupiter, three-dimensional space, effect of the other planets), as will become clear in the following.

We assume that Jupiter revolves around the Sun in a circular orbit and we consider a uniformly rotating frame of reference xOy , on the plane of motion, whose origin is the center of mass of Sun and Jupiter and the x -axis is the Sun–Jupiter line. If we choose the unit of mass to be the sum of the masses of Sun and Jupiter, the length unit to be equal to the (fixed) distance between Sun and Jupiter and $G = 1$, then the revolution period of Jupiter is $T = 2\pi$. It can be proved that there exists, in the above rotating frame, a family of nearly circular periodic orbits of the asteroid, along which the semimajor axis, and consequently the ratio n/n' , vary continuously, where $n(n')$ is the orbital frequency of the asteroid (Jupiter). At the points where n/n' is rational (except for $n/n' = (p + 1)/p$) we have a bifurcation of a family of resonant

periodic orbits of the asteroid, along which the resonance n/n' remains almost constant and the eccentricity of the asteroid increases, starting from zero. On this resonant family exist both stable and unstable orbits (see, e.g., Hadjidemetriou 1992).

We shall focus our attention on the case $n/n' = 12/7$. At this resonance there exists a family of resonant periodic orbits, in the rotating frame, symmetric with respect to the x -axis. The initial conditions of a periodic orbit are $x(0)$, $y(0) = 0$, $\dot{x}(0) = 0$, $\dot{y}(0)$ and the period is very close to the unperturbed value, $T = 7 \times 2\pi = 14\pi$. In Fig. 1a we present this resonant family in the space $x(0)$ -energy (E , instead of $\dot{y}(0)$) and in Fig. 1b in the space $x(0)$ - T . The circular family, from which the resonant family bifurcates, is also shown. In the above-mentioned normalized units the semimajor axis of an asteroid initially on the 12:7 resonance is close to the value $a = 0.698$. There are two branches of the resonant family that bifurcate from the circular family. In one of them the asteroid is initially at perihelion and in the other at aphelion. In particular, there are in both branches Helga-like orbits, with eccentricities close to the value 0.0761 (which is the

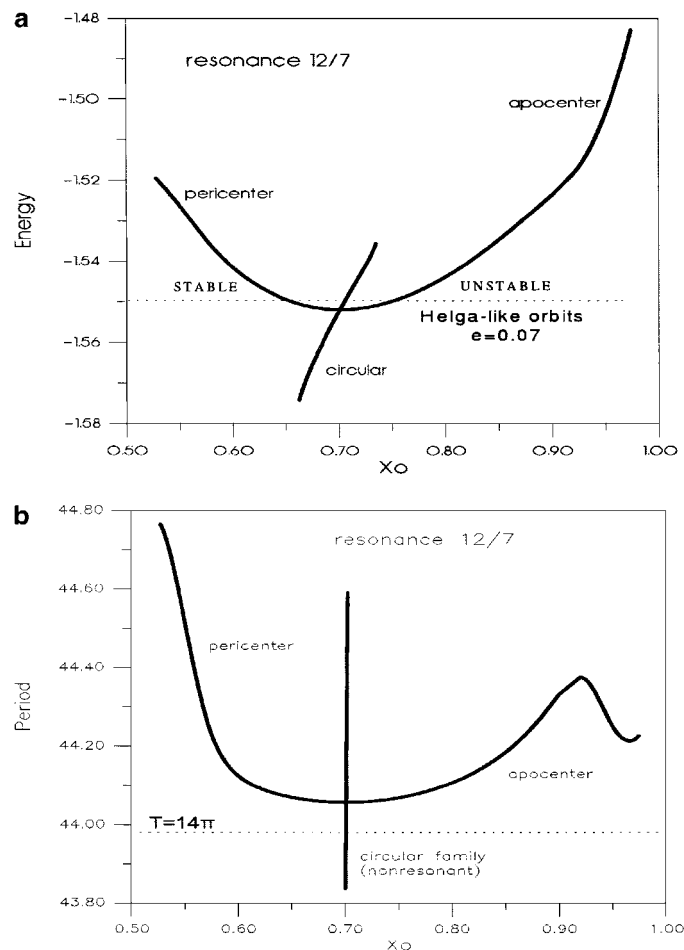


FIG. 1. (a) The family of resonant 12/7 periodic orbits in the $x(0)$ -Energy space. The line $E = -1.55010966$ corresponds to Helga-like orbits. (b) The same family in the $x(0)$ - T space. There does not exist any orbit with period equal to $T = 14\pi$.

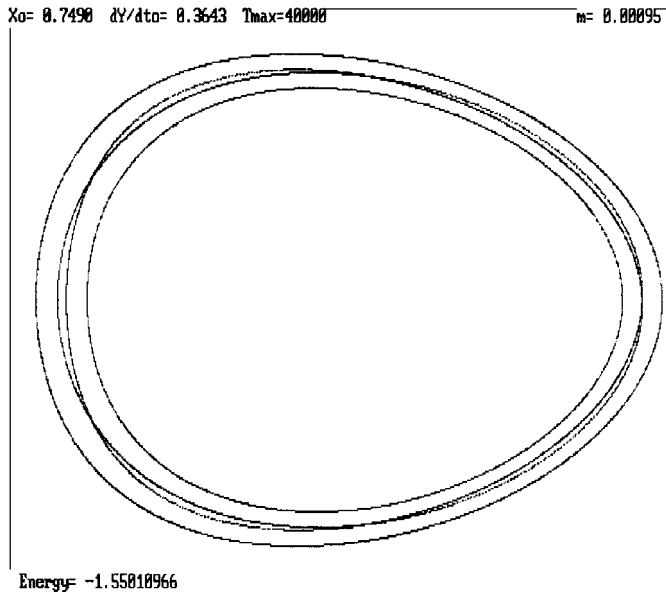


FIG. 2. A Poincaré surface of section for the Helga-like orbits in the CPRTBP.

initial value of eccentricity used in our numerical experiments). The apocentric orbits are unstable and the pericentric orbits are stable.

The structure of the phase space is clearly seen if we take the Poincaré mapping on the surface of section $y(0) = 0$, $E = \text{const}$. For Helga-like orbits we have the surface of section shown in Fig. 2 for $E = -1.55010966$. We see that there are two sets of periodic orbits,¹ one stable (at $\sigma = 0$, i.e., $\omega = 0$) and the other unstable (at $\sigma = \pi$, i.e., $\omega = \pi$). The characteristic exponent, γ , of the unstable periodic orbit has been calculated and corresponds to $\gamma^{-1} = 8000$ years. Note that the width of the libration region (island) is very small, so that a small deviation from the exact periodic orbit would result to a trajectory that comes close to both the stable and the unstable regions. This could generate chaotic motion, which would be confined in a narrow region of phase-space, bounded by smooth invariant curves. Thus, a phenomenon that could be characterized as *stable chaos* occurs naturally in the 12:7 resonance of the simplest model that describes asteroidal motion.

3.2. Elliptic Planar Restricted Three-Body Problem

Let us now assume that Jupiter moves on a fixed elliptic orbit. The dynamical evolution in this model depends on the structure of the phase space, which is defined by the fixed points that exist on a surface of section. These fixed points correspond to the resonant periodic orbits of the model. If no fixed points exist, no strong chaotic phenomena (e.g., sudden jumps in the eccentricity) are expected.

¹ These appear as a chain of five islands.

The role played by the fixed points in a model is clearly seen in the study of asteroidal motion in the 3:1 resonance (Hadjidemetriou 1993). In this case there are, in the elliptic model, two fixed points for small and two more for high eccentricity values. In a model where the high eccentricity resonances are absent (this is the case studied by Wisdom 1982, 1983), we have chaotic motion and sudden jumps of the eccentricity only up to $e = 0.3$. Beyond that region, the motion appears to be regular. If, however, we include the high eccentricity resonances in the model, the evolution changes drastically and jumps of the eccentricity of the asteroid up to 0.9 occur (Hadjidemetriou 1993). This phenomenon is due to the fact that the introduction of the high eccentricity fixed points (at $e = 0.80$) changes the topology of the model's phase space and the high eccentricity regions are no longer isolated by invariant tori.

In the 12:7 resonance there are no fixed points in the elliptic model for the following reason: A bifurcation of a family of periodic orbits from the circular to the elliptic model exists only if there is a periodic orbit on the family of the circular model (see Fig. 1) whose period is an exact multiple of 2π , in our case $T = 14\pi = 43.982297$. This is because the elliptic restricted three-body problem is a 2π -periodic time dependent dynamical system and any periodic orbit must have a period which is a multiple of the period 2π . However, from Fig. 1b it is clear that such an orbit does not exist (contrary to other resonances, e.g., 3:1, 2:1). This means that the low eccentricity regions of the phase space cannot be connected, through a single chaotic path, with the high eccentricity ones (however, since the stability of both the apocentric and pericentric branches changes with the eccentricity, there are bifurcations of higher multiplicity resonant periodic orbits). Thus, we come to the conclusion that in the 4D phase space of the planar elliptic problem at the 12:7 resonance no dramatic effects are expected in the evolution of an asteroid. The noncontinuation of the main family of periodic orbits offers in this sense a protection mechanism for the evolution of low-eccentricity orbits. We emphasize, however, that, in this part of the outer asteroid belt, the resonances are closely spaced. In fact, two low-order resonances, the 5:3 and 7:4 comensurabilities, lie on both sides of the 12:7 resonance and, even for moderate eccentricities ($e \sim 0.15$), their proximity should be important for the dynamical evolution of an asteroid.

3.3. More Advanced Models

The model used in our numerical experiments is, basically, the spatial elliptic restricted three-body problem. The differences between the planar case and the spatial case cannot lead to dramatic changes, at least for nearly coplanar orbits, which is the case in our numerical experiments. Including more planets in the model would result in an increase of the perturbations induced to the asteroid's orbit. The most important changes come from the fact that the orbit of Jupiter (as well as of the rest of the planets) is not fixed any more but is secularly precessing.

The frequencies describing the precession of the planetary orbits constitute the set of *secular frequencies* of the Solar System.

A resonance between the precession frequency of an asteroid's longitude of perihelion (or node) and one (or a linear combination) of the secular frequencies is called a *secular resonance*. The role played by secular resonances in the formation of the Kirkwood gaps and the dynamical transport of near-Earth asteroids (NEAs) has been proved to be extremely important (see, e.g., Moons 1997, Froeschlé 1997). Outside mean motion resonances, the location of the main secular resonances (up to order three) on the (a, i) plane can be found in Milani and Knezevic (1990) (see also Morbidelli and Henrard, 1991). For $a \sim 3.63$ and $e \sim 0.1$ the main secular resonances seem to be located at inclinations much larger than 4° , which is the mean inclination of Helga. The 12:7 resonance is probably too weak to significantly modify the proper frequency of the perihelion longitude, with respect to the nonresonant case. Thus, Helga-like orbits seem not to be affected by secular resonances and the differences between the elliptic three-body problem and N -body ($N > 3$) models are not expected to be dramatic for the case studied here.

4. NUMERICAL RESULTS

During the first 50 Myr of our simulations, the “true” Helga did not develop a Jupiter-crossing orbit. The evolution of its osculating semimajor axis and eccentricity during this time interval is shown in Figs. 3a and 3b. In the 5-Gyr integration, Helga remained in the same orbital elements' region for about 1.6 Gyr, whence it entered the action sphere of Jupiter. We also verified the fact that Helga evolves on a chaotic trajectory, with a Lyapunov time of about 6×10^3 years (see below Fig. 8). This chaotic behavior can be visualized in Fig. 3c, which shows the time evolution of the element $\Theta = 7\lambda - 12\lambda_J$, where periods of circulation in both directions are interspersed within short periods of libration. Using the standard notation of celestial mechanics, $\lambda = \Omega + \omega + M$ (λ_J is the mean longitude of the minor body (Jupiter)). These results are in agreement with the previously reported results of Milani and Nobili (1992) and Murray and Holman (1997).

4.1. Evolution of G1 and G2 in the ERTBP Model

The stability of the orbital elements for such a long time interval is not, however, the case for the majority of our test particles. On the contrary, as seen in Fig. 4a, the number of particles, $N(t)$, still orbiting the Sun on a non-Jupiter-crossing trajectory after time t decreases rapidly. Almost 60% of the particles leak out from the system, for both groups, on a 20-Myr time scale (see Table I). In Fig. 4a we have included the results for two smaller samples of particles, initially placed in the 7:4 and 5:3 resonance, respectively, for comparison. These two resonances lie on both sides of the 12:7 mean motion resonance. In Fig. 4b the same plot as in Fig. 4a is given for the particles of G2 and for $\Delta t = 50$ Myr. The percentage of escaping particles increases now to 71.3%. Fitting an exponential decay law of the form,

$$N(t) = N(0)e^{-\gamma t}, \quad (4)$$

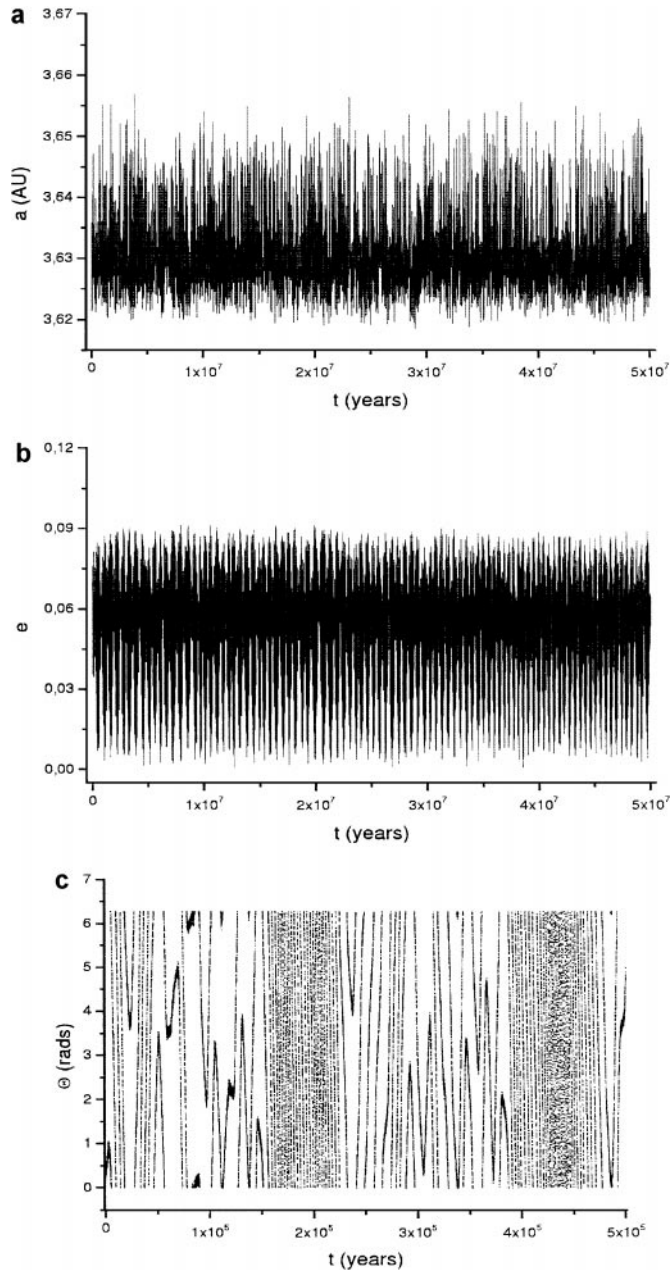


FIG. 3. Evolution of (a) the osculating semimajor axis and (b) the osculating eccentricity of the asteroid 522-Helga for $\Delta t = 50$ Myr. The evolution of the element $\Theta = 7\lambda - 12\lambda_J$ (c) is typical of a chaotic trajectory.

to this curve, we get $\gamma^{-1} = (16.3 \pm 0.8) \times 10^6$, but, as we see in the plot, the existence of *late escapers*, i.e., an almost linear “tail” of escaping particles with $T_E > 15$ Myr, spoils the fit. A modified exponential decay of the form,

$$N(t) = N_0 + N_1 e^{-\gamma t}, \quad (5)$$

with $\gamma^{-1} = (8.9 \pm 0.6) \times 10^6$ (which implies that a part— N_0 —of the initial population will not escape) fits the data in a much better way.

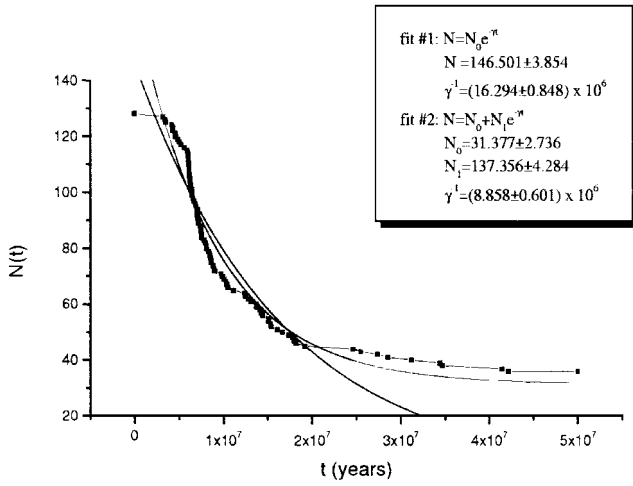
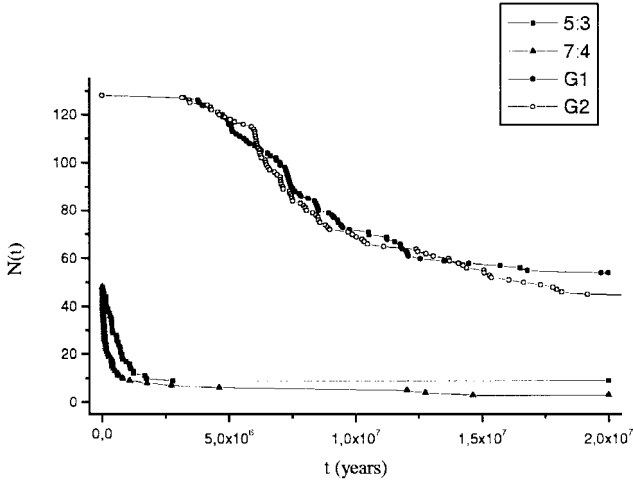


FIG. 4. (Top) The total number of particles still on resonance, $N(t)$, as a function of time ($\Delta t = 20$ Myr), for the four groups mentioned in the text. (Bottom) The same graph for G2 only and for $\Delta t = 50$ Myr, fitted by the two exponentials mentioned in the text.

The histogram of escape times for G2 is shown in Fig. 5. The mean escape time is about 6.5 Myr and the dispersion about the mean is about 3.5 Myr. If the escape time was not strongly depending on the initial conditions, this histogram should have

TABLE I
Escape Statistics in the ERTBP^a

Group	Escaping (%)	$\langle T_E \rangle$ (years)
7:4	93.75	7.2×10^4
5:3	81.25	6.3×10^5
G1	57.81	6.6×10^6
G2	64.34	6.4×10^6
G2*	70.54	5.4×10^6

^a The percentages are obtained after the 20-Myr integration for all groups except G2*, which is the percentage for G2 taken after 50 Myr.

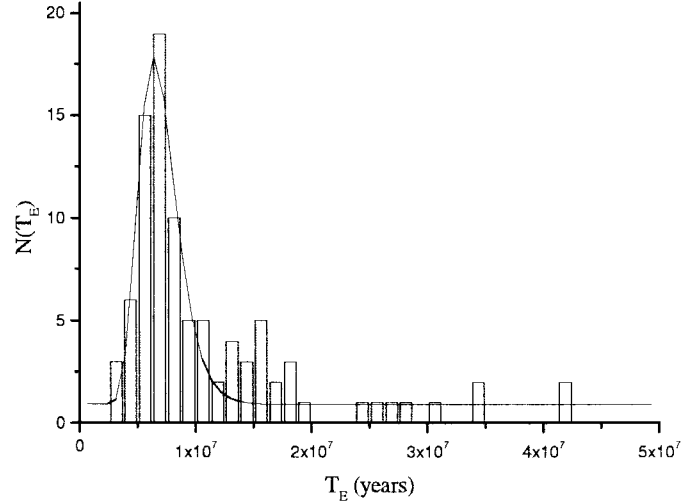


FIG. 5. The histogram of escape times for G2 ($\Delta t = 50$ Myr), binned to 1.25-Myr intervals. The fitted curve is a log-normal distribution.

the shape of a steep Gaussian distribution, i.e., a well defined mean value and a small dispersion, since all the particles would diffuse toward larger eccentricities at the same speed. Instead, we find that the histogram is best-fitted by a log-normal distribution, with a very long tail, something which is also the footprint of *Lévy-like random walks* (Shlesinger *et al.* 1993), which are nonclassical diffusive processes. Obviously, our “true” Helga lies in the far edge of the distribution’s tail.

The above results, clearly, depend upon the initial distribution of the test particles. Since the distribution is a δ -function of the actions and uniform in the angles ω and M , it is reasonable to imagine that there must be a relation between the escape time of an asteroid and its initial phases, which explains why some particles escape within a 10-Myr time scale while others may take as long as 2 Gyr to encounter Jupiter. Figure 6 shows this relation; let us present the initial conditions for the G2 particles on the (σ, ν) plane of *resonant arguments*,

$$\begin{aligned} \sigma &= \frac{12}{5} \lambda_J - \frac{7}{5} \lambda - \varpi \\ \nu &= -\frac{12}{5} \lambda_J + \frac{7}{5} \lambda + \varpi_J, \end{aligned} \quad (6)$$

where $\varpi = \omega + \Omega$ is the longitude of perihelion of the asteroid and ϖ_J that of Jupiter. As shown in this figure, the initial conditions of the particles that do not escape within the 50 Myr are not randomly distributed on the (σ, ν) plane but, instead, they are mostly concentrated around the diagonal, $\varpi - \varpi_J = 0$, of the plot. This set of surviving particles has initial perihelia in the range

$$\frac{9\pi}{8} \leq \omega_0 \leq \frac{14\pi}{8}, \quad (7)$$

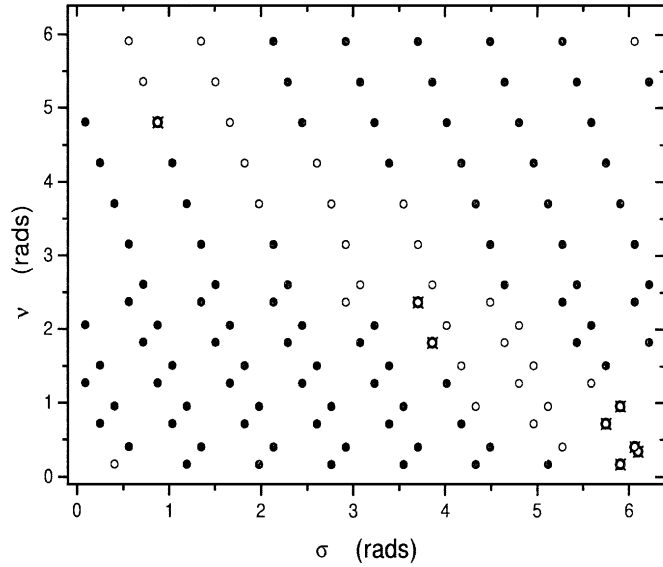


FIG. 6. The (σ, ν) plane of initial conditions. Filled circles represent initial conditions which lead to escape within 50 Myr. Open circles correspond to the set of initial conditions of the surviving population. Crossed circles denote the stable chaotic particles found. The plot is not uniform, since the initial distribution is set on a 16×8 grid in (ω, M) .

which corresponds to

$$-\frac{\pi}{3} < (\varpi - \varpi_J)_0 < \frac{\pi}{3}, \quad (8)$$

where the subscript zero refers to initial conditions.

The evolution of the orbits on the $(e, \varpi - \varpi_J)$ plane is shown, for some representative cases, in Fig. 7. It is clear from the plot that, for orbits which eventually escape (the first three orbits from top to bottom in Fig. 7a), the critical argument $\varpi - \varpi_J$ circulates and the eccentricity can reach values up to $e = 0.19$; the initial value $e = 0.0761$ is actually close to the minimum value of this osculating element. On the other hand, for all the orbits which do not escape within the 50-Myr time span, either the motion takes place very close to a narrow region of libration (like Helga, which is shown at the bottom of Fig. 7a) or the critical argument $\varpi - \varpi_J$ remains always in libration (Fig. 7b). For these orbits the initial eccentricity is close to the maximum value of $e(t)$ and the *proper eccentricity* should be of the order of the forced eccentricity ($e_J \simeq 0.048$). The Lyapunov exponent was calculated for the surviving particles and the results found can be summarized as follows:

(a) seven of them (the initial conditions are given in Table II) show *exactly* the same behavior as Helga; namely, they evolve on chaotic trajectories with $T_L \sim 6000$ years (Fig. 8) but their orbital elements have no significant variations over the 50-Myr time interval. Also, their Θ plots show exactly the same pattern; i.e., Θ is a slow variable alternating between circulation and libration (an example is shown in Fig. 9). Given these results, we can conclude that these fictitious asteroids exhibit the same kind

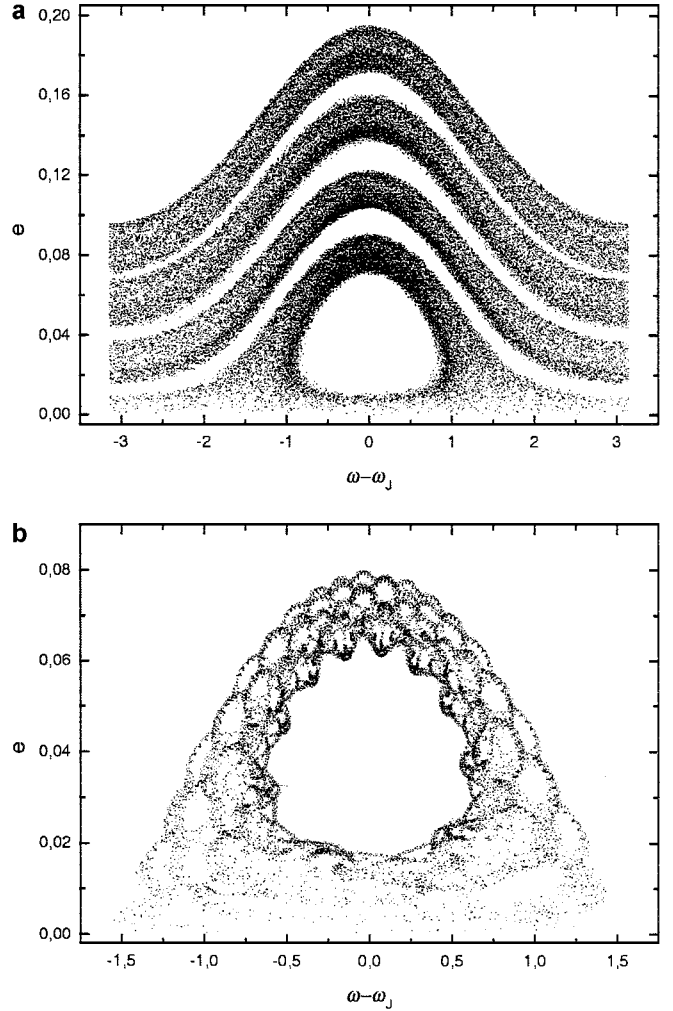


FIG. 7. Evolution of the orbits on the $(e, \varpi - \varpi_J)$ plane: (a) for escaping orbits (top three) $\varpi - \varpi_J$ circulates and the eccentricity reaches values up to $e = 0.19$ while for Helga-like orbits (bottom) $e \leq 0.1$ and the motion takes place very close to a small libration region. (b) An orbit for which $\varpi - \varpi_J$ remains always in libration and motion appears to be quasi-periodic.

of motion as Helga, i.e., *stable chaotic motion*. It is interesting that these orbits seem to gather to the borders of the “stable” (in the sense of orbital stability) set of initial conditions defined by Eq. (8).

TABLE II
Initial Conditions for G2 Particles in Stable Chaos

Particle	Ω_0 (rads)	M_0 (rads)	T_L (years)
1	$10\pi/8$	$2\pi/8$	5.1×10^3
2	$11\pi/8$	0	5.9×10^3
3	$11\pi/8$	$12\pi/8$	5.1×10^3
4	$12\pi/8$	$10\pi/8$	4.8×10^3
5	$12\pi/8$	$14\pi/8$	6.1×10^3
6	$13\pi/8$	$6\pi/8$	4.2×10^3
7	$13\pi/8$	$12\pi/8$	4.9×10^3

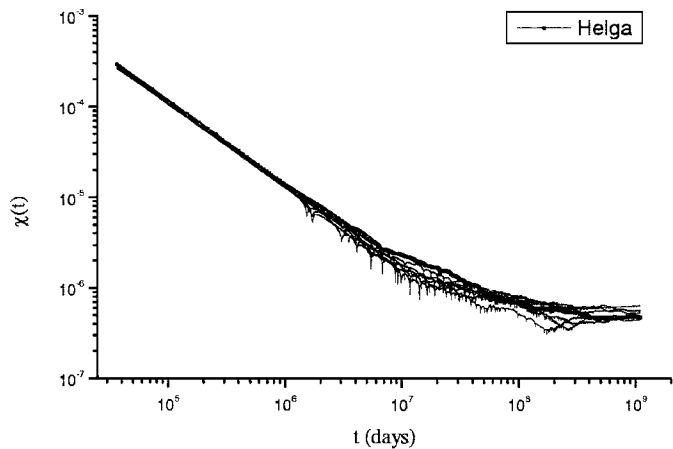


FIG. 8. Calculation of the Lyapunov exponent for the stable chaotic particles. All particles have Lyapunov times of the order of 6000 years.

(b) Among the surviving particles we also found chaotic orbits for which the Lyapunov time is larger than 10^5 years. We do not, however, classify them as stable chaos.

(c) For most of the surviving orbits a 10 Myr integration for the calculation of the Lyapunov exponent shows no signs of chaoticity; i.e., the divergence $\chi(t)$ decreases linearly on a log-log plot of t vs $\chi(t)$. Also, no evidence for chaos can be seen in the evolution of Θ , which always circulates. Thus, we have numerical indications that quasi-periodic orbits exist among the nonescaping orbits. The argument $\varpi - \varpi_J$ is librating for most of these orbits (one of them is shown in Fig. 7b).

It is known, however, that one cannot prove (but only disprove) the quasi-periodic nature of an orbit by means of numerical methods. It may be the case that at least some of the orbits mentioned in (c) could also be chaotic (like those mentioned in (b)) but they are stuck close to quasi-periodic orbits, thus behaving in a regular manner for very long time. A finer grid of initial conditions and longer integrations would be needed in order to obtain a detailed “Lyapunov map” of this “stable” set. In this respect stickiness indeed occurs in the vicinity of the 12:7 mean motion resonance. The question whether Helga, as well as the other stable chaotic orbits mentioned in (a), could also be considered as extreme cases of sticky orbits has not a simple answer. The fact that these orbits seem to emanate from the borders of the “stable” set admits such an interpretation. Also, as we will see in a following section, *all* the nonescaping orbits share a common property, namely a long-time correlated evolution of the eccentricity-related Delaunay actions. On the other hand, the evolution of the critical argument $\Theta = 7\lambda - 12\lambda_J$ is typical of clearly chaotic trajectories. This point will be further discussed in the final section of the paper.

In Fig. 10 the osculating semimajor axis and eccentricity time series of the fastest G2 escaper are shown. It is evident that the evolution of the osculating elements is very different from those of Helga and the other stable chaotic particles found. In particular, the eccentricity fluctuates with a maximum value of

about 0.17, much larger than the corresponding value for Helga-like orbits (which is about 0.1), and the amplitude of fluctuation is slowly increasing. At such values of e , overlapping with close-by resonances may be expected (see Dermott and Murray, 1983). At $t \approx 3.2$ Myr a sudden jump in eccentricity occurs, before the asteroid encounters Jupiter. As far as the semimajor axis is concerned, it is constantly drifting toward larger mean values, while the amplitude of its oscillations increases as well. This kind of evolution indicates that the asteroid is slowly driven into a close-by resonance which can pump the eccentricity up to

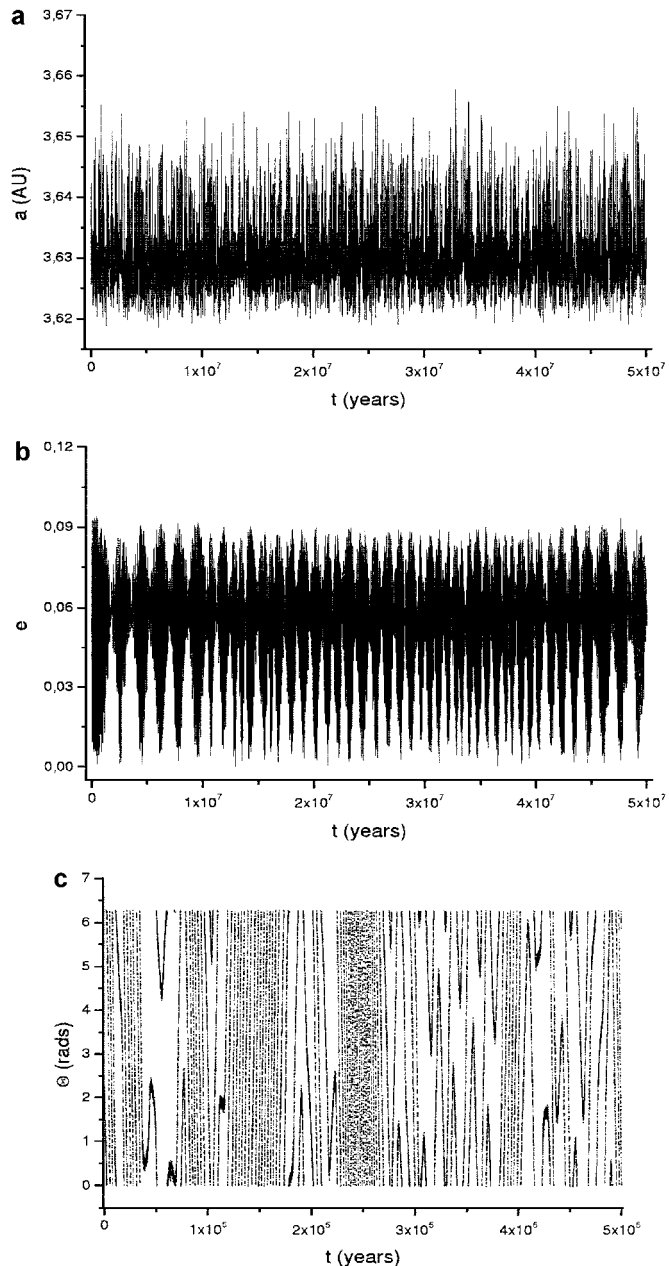


FIG. 9. Another example of stable chaos: (a) osculating semimajor axis, (b) osculating eccentricity, and (c) the element Θ . The behavior seen in this plot is exactly the same as in Fig. 3 for Helga.

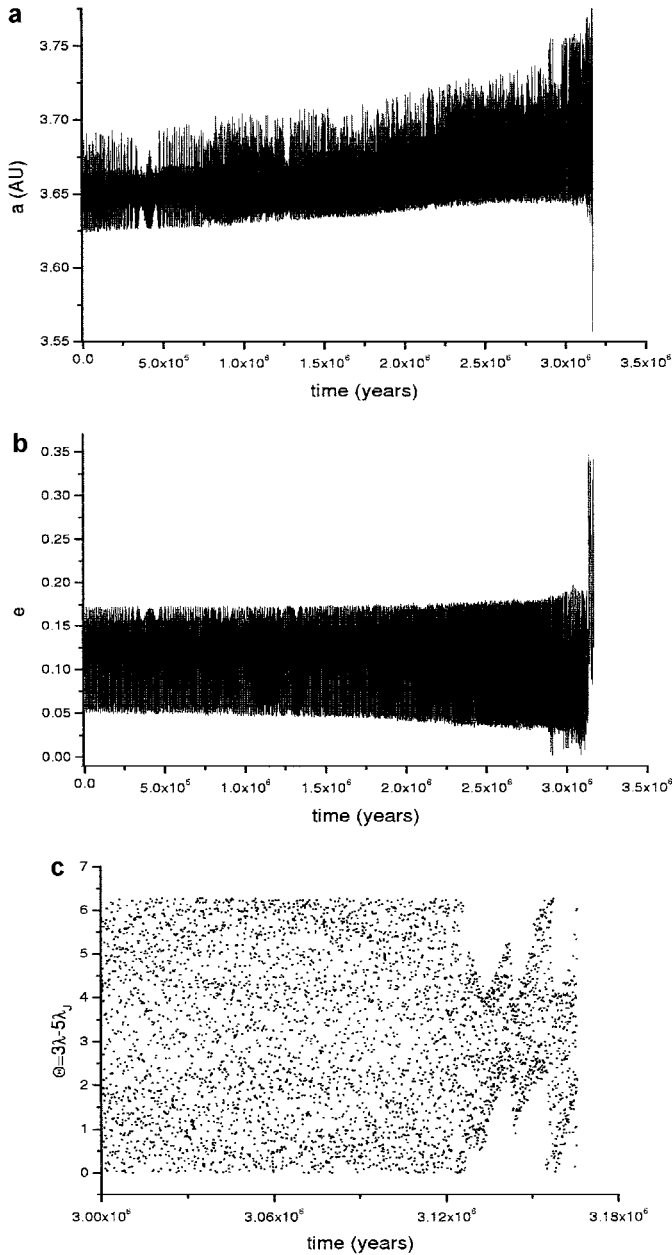


FIG. 10. The osculating semimajor axis (a) and eccentricity (b) time series of the fastest G2 escaper. The resonant argument $\Theta = 3\lambda - 5\lambda_J$ (c) shows a change from circulation to libration at $t \approx 3.15$ Myr.

Jupiter-crossing values. At $a \approx 3.7$ AU the strongest resonance present is the 5:3 mean motion resonance. The corresponding resonant argument, $\Theta = 3\lambda - 5\lambda_J$, is also shown in Fig. 10 for the interval 3–3.25 Myr. Θ is circulating up to $t \approx 3.15$ Myr and then changes to a libration, before the asteroid eventually escapes, indicating that this is indeed the case here.

4.2. Evolution of G2 in the 4P Model

As mentioned before, we also integrated the G2 particles (again for 50 Myr) in the four-planet configuration. This was

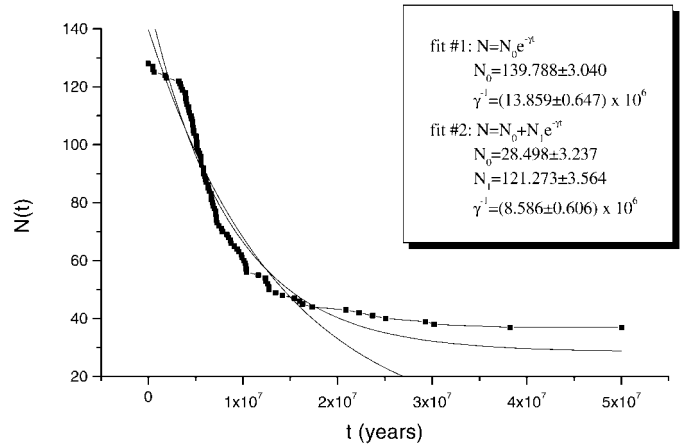


FIG. 11. Decay of the number of particles $N(t)$ for G2 in the 4P model ($\Delta t = 50$ Myr). Again two exponential fits are superimposed.

done in order to see how the additional perturbations induced by the interaction of the four giant planets modify the results that we found in the framework of the ERTBP. Figures 11, 12, and 13 are the counterparts of Figs. 4b, 5, and 6, respectively.

At a first glance, we see that the basic features of the previous plots are preserved in this case also. In particular, most of the particles again leak out from the system within 20 Myr, as seen in Fig. 11, and the histogram of escape times (Fig. 12) has again the shape of a log-normal distribution. Thus, although the escape times of individual particles are not the same any more, the statistical behavior of G2 is the same within the two models. The percentage of escaping particles does not change by much (see also Table I), but the mean escape time decreases to $\langle T_E \rangle \approx 5.4 \times 10^6$ years and the dispersion increases. This is expected, since the additional perturbations induced by the other planets speed up the diffusive process. However, as discussed in

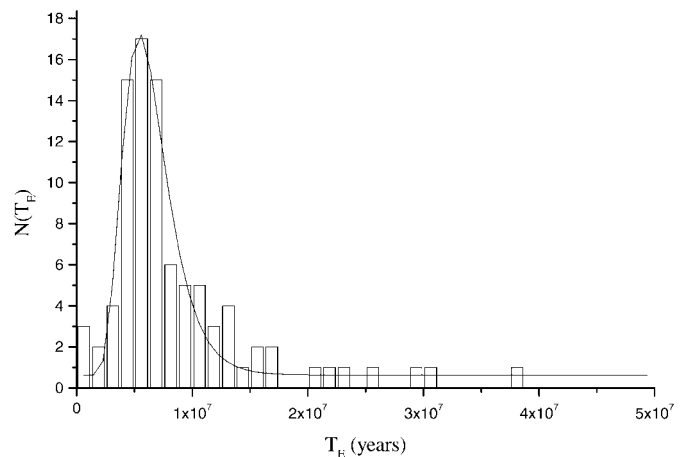


FIG. 12. The histogram of escape times for G2 in the 4P model ($\Delta t = 50$ Myr). The mean escape time is now approximately 5.5×10^6 years. The fitted curve is again a log-normal distribution.

Section 3, for such values of the semimajor axis the main secular resonances are located at much higher inclinations than the mean inclination of these asteroids ($i \sim 4^\circ$). Thus, the asteroids are not dynamically affected by them and the statistical behavior of the G2 set is the same within the two models.

Figure 13 is almost identical to Fig. 6. The $(\varpi - \varpi_J)_0$ channel of surviving particles is again present. The stable chaotic asteroids are again seen to emanate from the borders of a “stable” set of initial conditions. Figures 6 and 13 differ only in the boundaries of the initial perihelia set, which leads to regular motion, i.e., at $\omega_0 = 9\pi/8$ and $\omega_0 = 14\pi/8$. However, we stress here the fact that the exact differences between the two models, concerning the “stable” region, cannot be evaluated from the present results and a finer mesh of initial conditions has to be used for this purpose.

4.3. Stable Chaos and Long-Time Correlated Motion

The time series of the osculating elements of stable chaotic asteroids are characterized by a remarkable stationarity, as is also seen in Figs. 3 and 7. In fact, Milani *et al.* (1997) calculated proper elements (e_P and I_P) with almost undetectable diffusion for some stable chaotic asteroids. The situation is different for the chaotic particles which, eventually, escape. One of the tools used to distinguish between quasi-periodic and “random” time series is the *autocorrelation function*, $r(k)$, which measures how well correlated are two parts of the time series which are k time lags apart. For quasi-periodic signals, $r(k)$ is also quasi-periodic, while for chaotic (or random) time series $r(k)$ decays exponentially with time (or k). The time at which $r(k)$ drops below the value $1/e$ (without increasing again) is called the *autocorrelation time*, τ_C .

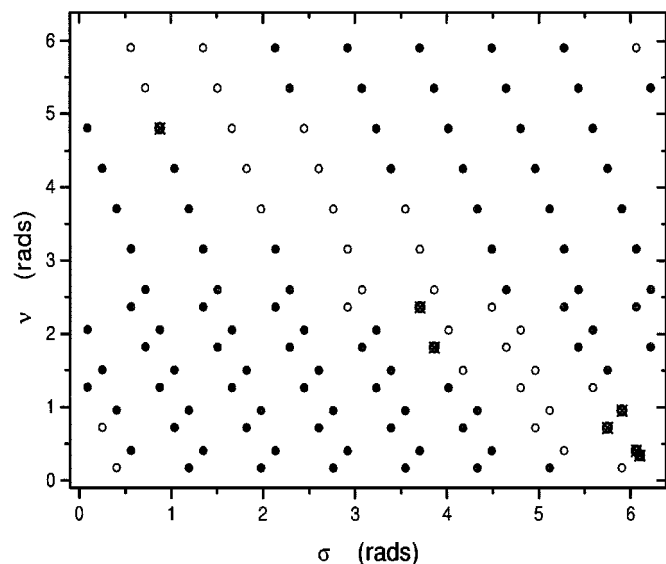


FIG. 13. The (σ, ν) plane of initial conditions for the 4P model. The symbols used are the same as in Fig. 6.

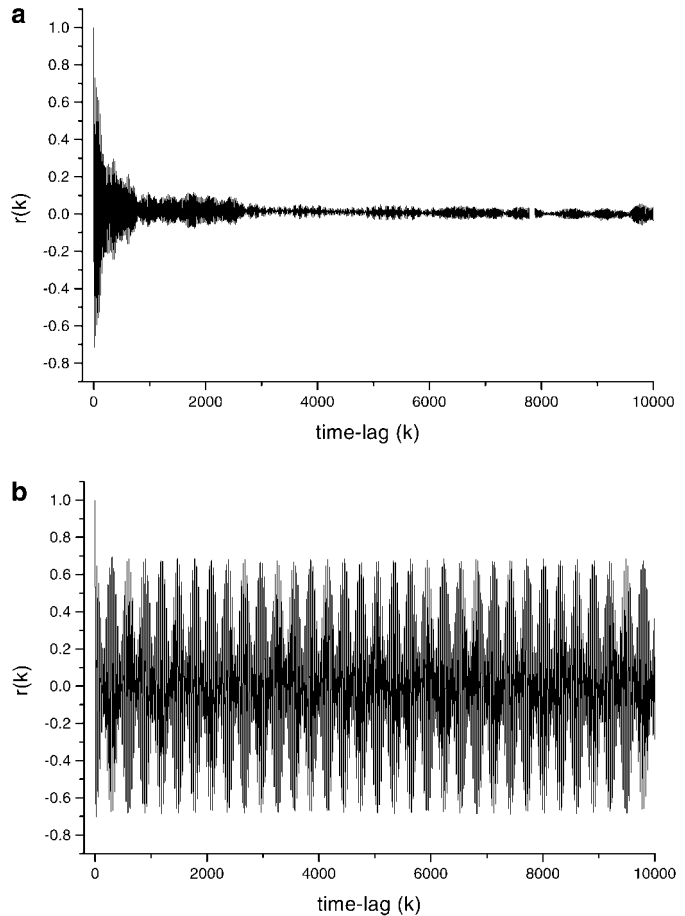


FIG. 14. The autocorrelation function, $r(k)$, as a function of the time lag, k . Fast decay of linear correlations is observed for the escapers (a), while for Helga (b) and the rest of the stable chaotic particles $r(k)$ remains almost constant.

We calculated $r(k)$ for both the $\mathcal{G}(t)$ and the $\mathcal{H}(t)$ action time series of all G2 particles, using the records of the first 3 Myr of our integration (in the ERTBP model). Since the inclinations do not change by much, the results for both time series are almost identical.² The results are very interesting. While for the chaotic particles which escape linear correlations decay exponentially with time, as they should, this is not true for the stable chaotic particles. In fact, $r(k)$ is almost quasi-periodic. A typical example is shown in Fig. 14, where we have plotted $r(k)$ for both an escaping particle and for 522-Helga.

Finding different autocorrelation times among the ejected particles tempted us to search for a possible relationship between the escape time, T_E , of asteroids and the autocorrelation time, τ_C , of their action time series. In Fig. 15 we have plotted τ_C against T_E for all the escaping particles of G2. A power-law fit yields the relation,

$$T_E = a\tau_C^b, \quad (9)$$

² Note, however, that this need not be the case in other regions of the asteroid belt.

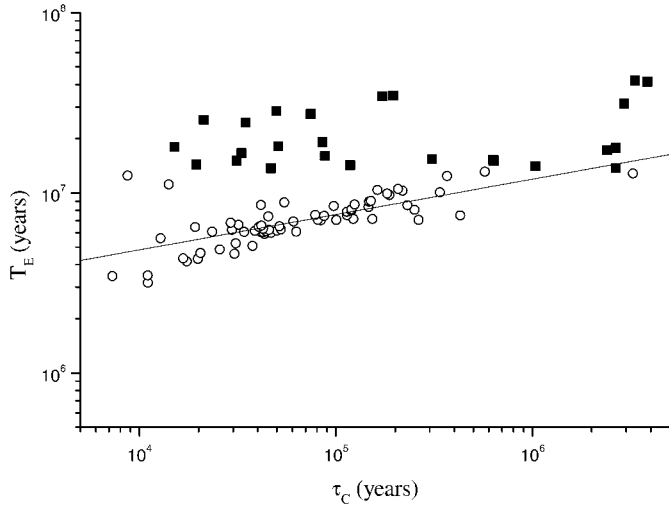


FIG. 15. A log-log plot of τ_C against T_E for all escaping particles of G2 (ERTBP). The power-law fit shown here, corresponding to the “bulge” of the escaping distribution (open circles), yields $T_E \sim \tau_C^{1/5}$. The population of “late escapers” is represented in this plot by filled circles.

with $a = (7.53 \pm 3.74) \times 10^5$ and $b = 0.221 \pm 0.035$. However, the correlation coefficient of the fit is rather low, namely $R = 0.55$. The “spoiling” of the fit is caused by the fact that there are, clearly, two populations on this plot. The larger one corresponds to particles which belong to the bulge of the escaping distribution seen in Fig. 5; i.e. $T_E \leq 13$ Myr (which is $2\sigma_{T_E}$ away from the mean), and the smaller population (about 30% of the total) is that of the distribution’s tail; i.e., $T_E \geq 13$ Myr. If one disregards the tail population, the resulting fit, describing only the bulk of the escaping distribution, is much better ($R = 0.72 \pm 0.09$ and $b = 0.196 \pm 0.024$). The late escapers (shown as black squares in Fig. 15) have, surprisingly, small autocorrelation times. However, one has to remember that the autocorrelation function, $r(k)$, measures the decay of linear correlations. Thus, $r(k)$ cannot detect any nonlinear correlations which may slow down the diffusion process for the late escapers.

5. CONCLUSIONS—DISCUSSION

In this paper we try to understand the nature of transport in the neighborhood of the 12:7 mean motion resonance and to interpret the peculiar orbital behavior of the asteroid 522-Helga. The peculiarity consists in the fact that Helga’s trajectory seems to be strongly chaotic—in terms of Lyapunov exponents—and yet the osculating elements of this asteroid remain stable for billions of years. Until now two different interpretations of this fact have appeared in the literature. Murison *et al.* (1994) proposed that the mean escape time from the 12:7 mean motion resonance is rather short and that Helga is the remnant of a much larger initial distribution of asteroids. In contrast, the analytic results of Murray and Holman (1997) indicate that the mean escape time from the 12:7 mean motion resonance is ex-

tremely long, so that Helga should not have initially too many partners. In the present paper we followed numerically the evolution of two initial distributions (G1 and G2). Both of them have a mean escape time of *about 7 Myr* (ERTBP), which is much shorter than the predictions of the analytic diffusive approximation of Murray and Holman (1997) for the planar case. Thus, although the simple power-law relation between T_L and T_E found by Lecar *et al.* (1992) may not hold, the conjecture of Murison *et al.* (1994) that 522-Helga is the remnant of a much larger distribution of asteroids that have already escaped from the Solar System may, in fact, be true. On the other hand, not all chaotic particles have similar escape times. In fact, T_E may vary by several orders of magnitude (in both the ERTBP and the 4P models), as shown clearly by the shape of the escaping distribution. More precisely, the percentage of late escapers, for which $T_E > \langle T_E \rangle + 2\sigma_{T_E} \approx 13$ Myr, is about 30% of the total escaping population. Thus, although all particles begin with the same action values, diffusion is much slower for a statistically significant percentage of them.

It seems that the key to understanding the conflicting results mentioned above is the underlying relation between the escape time of a test particle and its initial phase $\varpi - \varpi_J$. Milani and Nobili (1992) argued that the behavior of Helga can be explained as the result of a protection mechanism, which is not due to the resonance responsible for chaos, but is related to the behavior of the critical argument $\varpi - \varpi_J$ and the small value of Helga’s proper eccentricity. Our numerical results show, indeed, that all orbits which survive for 50 Myr are either performing librations in $\varpi - \varpi_J$ or cover a region of the $(e, \varpi - \varpi_J)$ plane just outside this narrow libration zone. For these orbits the initial eccentricity value ($e = 0.0761$) is close to the maximum osculating eccentricity and the proper eccentricity should be of the order of the forced eccentricity (e_J). However, we argue that this behavior is, in fact, related to the peculiarity of the 12:7 resonance stated in Section 3; i.e., the noncontinuation of the main family of periodic orbits in the planar elliptic problem. In other resonances (e.g., 3:1) the main unstable periodic orbit divides the XY plane ($X = e \cos(\varpi - \varpi_J)$, $Y = e \sin(\varpi - \varpi_J)$) into three topologically distinct regions (libration–internal circulation–external circulation) and this topology is responsible for the transport of initially low-eccentric orbits to high-eccentricity regions. This is evidently not the case for the 12:7 resonance; only a narrow libration zone with proper eccentricities less than 0.05 (like in Fig. 7b) exists while most of the orbits circulate. For those orbits which eventually escape, the proper eccentricity should be larger than 0.1. Helga-like orbits also circulate but with $e_p \sim 0.05$. Whether this mechanism is also present in other high-order resonances, which appear to be associated to the occurrence of stable chaos in the inner part of the asteroid belt, is certainly within our plans for future work. However, at this specific region of the outer belt studied in this paper, the resonances are closely spaced and, thus, overlap with adjacent low-order resonances can drive asteroids with initially moderate eccentricities

($0.1 \leq e \leq 0.15$) to Jupiter-crossing orbits, as shown in our results.

In the more general framework of Hamiltonian dynamics, the conjecture that stable chaos may be interpreted as a realization of the stickiness phenomenon seems appealing; the idea of testing the validity of this proposition led us to the work presented in this paper. Unfortunately the results are not conclusive enough. The fact that chaotic orbits seem to coexist (within the “stable” set defined by Eq. (8)) with quasi-periodic orbits implies that sticky orbits exist in this region; this characterization can certainly be given to those chaotic orbits found having large T_L s. The facts that (a) Helga-like orbits are seen to gather to the borders of this “stable” set and (b) these orbits, too, retain correlations in the eccentricity-related time series for times much longer than the corresponding T_L , support the idea that stable chaotic orbits may be considered as extreme (small T_L s) cases of stickiness. On the other hand, one would expect that the evolution of the critical argument, Θ , should be quite similar to that of quasi-periodic orbits for very long times, and this is not the case here. Therefore, we are tempted to conclude that, according to the protection mechanism described in Section 3 (and the previous paragraph), invariant tori may in fact be responsible for bounding the eccentricity of Helga-like orbits. These tori would form a hardly permeable barrier, even though we are dealing with a more-than-three degrees of freedom dynamical system. The question now is what we can define as stickiness: if the term is to be used for orbits winding around stable KAM tori (in the form of the counterparts of resonant islands in 2D) immersed in a mostly stochastic region, our results are in conflict. If, on the other hand, we use the same term to describe chaotic orbits within narrow stochastic layers which are “bounded” by “rotational” KAM curves (in the sense described above), the results are in agreement. Both situations can be responsible for the slow (subdiffusive) evolution of the eccentricity-related actions that we observe. Whether KAM tori can still persist under the perturbing effects of more-than-one planet (or they deform into the analog of *cantori*) is something that cannot be answered with the numerical results presented here. In any case, we must consider the fact that very little is known about stickiness (and the behavior of the different degrees of freedom of sticky orbits) in the phase space of dynamical systems of high dimensionality. It appears, therefore, that this complicated phenomenon is still a matter of investigation. For the specific case of stable chaos studied in this paper, much larger initial distributions of particles, including variations in Ω and the initial values of the actions, have to be integrated in order to examine the detailed structure of the “stable” set.

In any of the cases discussed above, the phrase *a random walk in the actions*, frequently used to describe chaotic variations of the orbital elements of asteroids, does not apply to Helga. In fact, all stable chaotic particles found in our integrations, unlike those which escape, do not respect one of the most fundamental properties of classic random walks, i.e., the exponential decay of linear correlations. This could be a characteristic of all asteroids

exhibiting stable chaos and we plan to test for this property other stable chaotic asteroids that have been discovered so far (Milani *et al.* 1997, Sidlichovsky 1998). The fact that stable chaotic particles, although having small Lyapunov times, retain correlations in the actions for a very long time is also an observation which leads to the conclusion that stable chaotic trajectories constitute a different “class” of dynamical objects. We argue that the property of nondecaying correlations could be used as a method to distinguish between fast escapers and stable chaos using short-time integrations. Such a method would consist of calculating both the Lyapunov exponent, λ , and the autocorrelation function of an action-like time series. Of course, it is also easy to distinguish between stable-chaotic and regular orbits, both of which retain correlations, by plotting the corresponding critical argument.

Slow decay of correlations is a characteristic of trajectories for which mixing in phase space may take an extremely long time (see Zaslavsky 1985). This is noted also in Yannacopoulos and Rowlands (1997), where the authors show how the *phase-randomization approximation* breaks down in the vicinity of stable orbits, even for large stochasticity parameters. In particular, these authors have shown that, in the case of area preserving maps on the plane, the quasi-linear approximation of the diffusion coefficient, D_{QL} , breaks down even above the critical threshold. This means that not only D becomes action dependent, but also that the value of $\langle(\Delta I)^2\rangle/\tau$ needs to be calculated at different τ s for different initial action values, depending on the measure of invariant sets contained within a given phase-space domain (which measure is not known a priori). Thus, the local structure of the phase space, as also suggested from our results, is very important for the mixing properties of the specific phase-space region and this, in turn, plays a key role in the proper formulation of a diffusive approximation.

On the other hand, the autocorrelation function decays quickly for all the escaping particles found in the simulations. The different autocorrelation times found for the ejected particles tempted us to search for a possible “statistical law,” connecting the autocorrelation time, τ_C , to the escape time, T_E . Unfortunately, a clear picture cannot be established with the results of only the present work. This is not only because of the small number of “asteroids,” but also because two populations of chaotic escapers seem to exist. The larger one, belonging to the bulk of the escaping distribution, can be described by a relation of the form $T_E \sim \tau_C^{1/5}$ rather well. However, trying to fit the whole escaping distribution does not give promising results. This is due to the second (smaller) population, which consists of *late escapers* with very short autocorrelation times. One has to remember, though, that $r(k)$ measures linear correlations and, thus, any nonlinear correlations that may slow down the diffusion process for these particles cannot be explored using this tool. More refined nonlinear tools have to be used in order to prove, or disprove, the existence of a statistical law connecting the escape time to the time of decorrelation of the eccentricity-related actions.

ACKNOWLEDGMENTS

The authors thank Alessandro Morbidelli and Andrea Milani for their critical remarks on the first draft of this paper. Also we thank Alessandro Morbidelli for recommending the SWIFT package. Many thanks to Hal Levison and Martin Duncan, the authors of SWIFT, for their help in using this integration package. This work was completed while K.T. was under a grant from the State Scholarship Foundation of Greece (IKY).

REFERENCES

- Aubry, S. 1978. The new concept of transitions by breaking of analyticity in a crystallographic model. In *Solitons and Condensed Matter Physics* (A. R. Bishop and T. Schneider, Eds.), pp. 264–277. Springer, Berlin.
- Dermott, S. F., and C. D. Murray 1983. Nature of the Kirkwood gaps in the asteroid belt. *Nature* **301**, 201–205.
- Froeschlé, Ch. 1997. Dynamical transport to planet-crossing orbits. In *The Dynamical Behaviour of Our Planetary System* (R. Dvorak and J. Henrard, Eds.), pp. 165–174. Kluwer Academic, Dordrecht.
- Hadjidemetriou, J. D. 1992. Resonant motion in the restricted three-body problem. *Celest. Mech. Dynam. Astron.* **56**, 201–219.
- Hadjidemetriou, J. D. 1993. Asteroid motion near the 3:1 resonance. *Celest. Mech. Dynam. Astron.* **56**, 563–599.
- Hadjidemetriou, J. D. 1995. Mechanisms of generation of chaos in the Solar System. In *From Newton to Chaos* (A. E. Roy, Ed.), pp. 79–96. Plenum, New York.
- Hadjidemetriou, J. D., and A. Lemaitre 1997. Asteroid motion Near the 2/1 resonance: A symplectic mapping approach. In *The Dynamical Behavior of Our Planetary System* (R. Dvorak and J. Henrard, Eds.), pp. 277–290. Kluwer Academic, Dordrecht.
- Holman, M., and N. Murray 1996. Chaos in high-order mean motion resonances in the outer asteroid belt. *Astron. J.* **112**, 1278–1293.
- Konishi, T. 1989. Relaxation and diffusion in Hamiltonian systems with many degrees of freedom. *Prog. Theor. Phys. Suppl.* **98**, 19–35.
- Lecar, M., F. Franklin, and M. Murison 1992. On predicting long term orbital instability—A relation between the Lyapunov time and sudden orbital transitions. *Astron. J.* **104**, 1230–1236.
- Levison, H., and M. Duncan 1994. The long-term dynamical behavior of short period comets. *Icarus* **108**, 18–36.
- Milani, A., and Z. Kenzevic 1990. Secular perturbation theory and computation of asteroid proper elements. *Celest. Mech. Dynam. Astron.* **49**, 247–411.
- Milani, A., and A. M. Nobili 1992. An example of stable chaos in the Solar System. *Nature* **357**, 569–571.
- Milani, A., A. Nobili, and Z. Knezevic 1997. Stable Chaos in the asteroid belt. *Icarus* **125**, 13–31.
- Moons, M. 1997. Review of the dynamics in the Kirkwood gaps. In *The Dynamical Behaviour of Our Planetary System* (R. Dvorak and J. Henrard, Eds.), pp. 175–204. Kluwer Academic, Dordrecht.
- Morbidelli, A., and C. Froeschlé 1996. On the relationship between Lyapunov times and macroscopic instability times. *Celest. Mech. Dynam. Astron.* **63**, 227–239.
- Morbidelli, A., and J. Henrard 1991. Secular resonances in the asteroid belt: Theoretical perturbation approach and the problem of their location. *Celest. Mech. Dynam. Astron.* **51**, 131–167.
- Murison, M., M. Lecar, and F. Franklin 1994. Chaotic motion in the outer asteroid belt and its relation to the age of the Solar System. *Astron. J.* **108**, 2323–2329.
- Murray, N., and M. Holman 1997. Diffusive chaos in the outer asteroid belt. *Astron. J.* **114**, 1246–1259.
- Percival, I. C. 1979. Variational principles for invariant tori and cantori. In *Nonlinear Dynamics and the Beam Beam Interaction* (M. Month and J. C. Herrera, Eds.), pp. 302–310, AIP Conf. Proc. 57. Woodbury, NY.
- Sidlichovsky, M. 1999. On stable chaos in the asteroid belt. *Celest. Mech. Dynam. Astron.* **73**, 77–86.
- Shlesinger, M. F., G. M. Zaslavsky, and J. Klafter 1993. Strange kinetics. *Nature* **363**, 31–37.
- Varvoglis, H., and A. Anastasiadis 1996. Transport in Hamiltonian systems and its relationship to the Lyapunov time. *Astron. J.* **111**, 1718–1720.
- Wisdom, J. 1982. The origin of Kirkwood gaps. *Astron. J.* **87**, 577–593.
- Wisdom, J. 1983. Chaotic behavior and the origin of the 3/1 Kirkwood gap. *Icarus* **56**, 51–74.
- Yannacopoulos, A. N., and G. Rowlands 1997. Local transport coefficients for chaotic systems. *J. Phys. A* **30**, 1503–1525.
- Zaslavsky, G. M. 1985. *Chaos in Dynamic Systems*. Harwood Academic, OPA, Amsterdam. [translated by V. I. Kisin].
- Zaslavsky, G. 1994. Fractional kinetic equation for Hamiltonian chaos. *Physica D* **76**, 110–122.